

Calculation of the potential for interaction of particles with complex atomic structures

E. Bagli,¹ V. Guidi,¹ and V. A. Maishev²¹*INFN Sezione di Ferrara and Dipartimento di Fisica, Università degli Studi di Ferrara, Via Saragat 1, 44100 Ferrara, Italy*²*Institute for High Energy Physics, 142281 Protvino, Russia*

(Received 28 October 2009; published 19 February 2010)

We present a method for calculation of the potential and related physical quantities experienced by a particle traversing an aligned periodic complex atomic structure. Classical physics equations and the expansion of periodic functions as a Fourier series have been used for the calculation. Based on this method, we have developed the ECHARM program, which calculates one- and two-dimensional averaged physical quantities of interest along the main axes of any orthorhombic and tetragonal structure. For the case of cubic symmetry, the calculation holds for any orientation. Complex structures such as zeolites have been worked out to show the capability of the program.

DOI: [10.1103/PhysRevE.81.026708](https://doi.org/10.1103/PhysRevE.81.026708)

PACS number(s): 02.60.-x, 61.85.+p, 71.15.-m

I. INTRODUCTION

Interaction of either charged or neutral particles with crystals is an area of science under development because of a wealth of applications with the particle energy spanning over several decades. Low- and medium-energy interactions of charged particles involve plasma etching [1] and plasma surface interaction in nuclear fusion facilities [2]. High-energy applications involve emission of many types of coherent radiation [3] and particle steering in bent crystals [3–6] via either channeling or volume reflection [7,8]. Important examples of interaction of neutral particles in crystals are the production of electron-positron pairs and birefringence of high energy gamma quanta [9,10]. More recently interaction of particles with nanostructures has met the interest of scientists [11].

For most experiments and applications, especially those pertaining to radiation emission and particle steering, silicon has been the base material because of the high perfection and ease of availability of currently produced monocrystals as wafers or ingots. Indeed, experiments have been made with other monocrystalline materials, such as Ge [12] and W [13], and also been proposed with new periodic complex atomic structures [14–16]. The discovery of novel effects is strongly related to the possibility to produce crystals with proper characteristics and to simulate their behavior. For the new materials, it arises the need for a methodology to calculate the physical quantities of interest.

As Lindhard showed [17], the motion of relativistic charged particles under channeling condition is well approximated with classical physics equations and, as a consequence, also the potential and its related quantities. A traditional approach for its calculation relies on the analytical representation of the screened Coulomb potential [16,18–20], for which its average is made for planar and axial cases by taking into consideration the potential of the atoms lying in neighboring planes or axes.

Another possible approach is based on the expansion in Fourier series of the physical quantities of interest. Although this approach has been widely used in many research areas, for the case of channeling it has been developed to date only for particular monoatomic cubic crystals along major orien-

tation [15,21–23]. The method based on Fourier expansion is more flexible than the former, inasmuch as it can be applied to any realistic model of the atomic potential. Moreover, it allows one to determine averaged one- and two-dimensional physical quantities for any axis and plane of the crystal.

In this paper we propose a complete treatment and generalization of the method based on the expansion of the electric potential as a Fourier series, which allows one to calculate the physical quantities of interest even in complex atomic structures. The method will be shown to determine the physical quantities with good approximations and with reasonable calculation time. Moreover, x-ray measurements of electron density can be directly used for more precise calculations of the potential. Finally the method of calculation has been implemented in a simulation code (the ECHARM program) for fast calculation even for a nonexpert user.

II. POTENTIAL AND RELATED QUANTITIES IN A PERIODIC STRUCTURE

Although the method of the Fourier expansion of the potential has already been used for some specific applications [15,21–23], its full detail has not been shown. In the following paragraphs we will highlight its main features and arrive at the expression for the potential.

A. General background

Three-dimensional periodic atomic structure is determined by the primitive cell and its basis; through the translation vectors \mathbf{a}_1 , \mathbf{a}_2 , \mathbf{a}_3 , one can build the whole atomic structure. Translation vector is defined as

$$\mathbf{r}_{\mathbf{k}} = k_1 \mathbf{a}_1 + k_2 \mathbf{a}_2 + k_3 \mathbf{a}_3, \quad (1)$$

where $\mathbf{k}=(k_1, k_2, k_3)$ is a set of integer numbers. In this first paragraph we consider for simplicity a perfect monoatomic structure without thermal vibrations. Let $u(\mathbf{r})$ be a scalar function determined in the space and the integral $\int_V u(\mathbf{r}) d\mathbf{r}$ be convergent over the whole space, then the function,

$$U(\mathbf{r}) = \sum_{\mathbf{k}} \sum_{j=1}^{N_0} u(\mathbf{r} - \mathbf{r}_{\mathbf{k}} - \mathbf{r}_j) \quad (2)$$

can be represented by its Fourier transform, \mathbf{r}_j being the coordinates of the j th atom in the primitive cell and N_0 the number of atoms in it,

$$\mathcal{U}(\mathbf{q}) = \int_V \mathcal{U}(\mathbf{r}) e^{i\mathbf{q}\cdot\mathbf{r}} d\mathbf{r} = \sum_{\mathbf{k}} \sum_{j=1}^{N_0} u(\mathbf{q}) e^{i\mathbf{q}\cdot(\mathbf{r}_k+\mathbf{r}_j)}, \quad (3)$$

where integration is made over the whole space V and where $u(\mathbf{q}) = \int_V u(\mathbf{r}) e^{i\mathbf{q}\cdot\mathbf{r}} d\mathbf{r}$. Using the δ function properties we obtain

$$\mathcal{U}(\mathbf{q}) = \frac{(2\pi)^3}{\Delta} \sum_{j=1}^{N_0} e^{i\mathbf{q}\cdot\mathbf{r}_j} \sum_{\mathbf{g}} u(\mathbf{q}) \delta(\mathbf{q} - \mathbf{g}), \quad (4)$$

where \mathbf{g} are the reciprocal lattice vectors [24]. By performing the reverse Fourier transform we get

$$\mathcal{U}(\mathbf{r}) = \frac{1}{\Delta} \sum_{\mathbf{g}} u(\mathbf{g}) S(\mathbf{g}) e^{-i\mathbf{g}\cdot\mathbf{r}}, \quad (5)$$

where Δ is the volume of the primitive cell and $S(\mathbf{g}) = \sum_{j=1}^{N_0} e^{i\mathbf{g}\cdot\mathbf{r}_j}$ is the structure factor.

The term with $\mathbf{g}=0$ in this sum equals to

$$\frac{1}{\Delta} u(\mathbf{g}=0) S(\mathbf{g}=0) = \frac{N_0}{\Delta} \int u(\mathbf{r}) d\mathbf{r}. \quad (6)$$

B. Case of an ideal structure

Let us approximate the potential of a complex periodic atomic structure as a sum of single-atom potential,

$$\varphi(\mathbf{r}) \approx \sum_{\mathbf{k}} \sum_{j=1}^{N_0} u(\mathbf{r} - \mathbf{r}_k - \mathbf{r}_j), \quad (7)$$

where $u(\mathbf{r})$ is the potential of an isolated atom. This formula does not consider the delocalization of electrons among neighboring atoms, though the x-ray experiments show that approximation is very good [24]. With the aim of investigating the interaction of relativistic particles with such structures, there is no need for a more precise description of the potential. We can rewrite the formula by using the expansion shown in previous section,

$$\varphi(\mathbf{r}) = \frac{1}{\Delta} \sum_{\mathbf{g}} u(\mathbf{g}) S(\mathbf{g}) e^{-i\mathbf{g}\cdot\mathbf{r}}. \quad (8)$$

By performing the Fourier transform of the Poisson equation to express $u(\mathbf{g})$, we obtain,

$$\varphi(\mathbf{r}) = \frac{4\pi e Z}{\Delta} \sum_{\mathbf{g} \neq 0} S(\mathbf{g}) \frac{[1 - F(\mathbf{g})]}{g^2} e^{-i\mathbf{g}\cdot\mathbf{r}}, \quad (9)$$

where e is the elementary charge, Z is the atomic number and $F(\mathbf{g})$ is the atomic form factor. We subtracted the term with $\mathbf{g}=0$ because the potential is defined except for an additive constant.

With the same procedure we can study the case of a polyatomic structure as a superposition of N independent monoatomic structures. Every structure have the same primitive

cell and the same main period, but, in general, different bases consisting of all the atoms with identical species.

$$\varphi(\mathbf{r}) = \sum_{l=1}^N \varphi_l(\mathbf{r}), \quad (10)$$

where l runs over the N atomic species. As a result, for the periodic polyatomic structures, it holds

$$\varphi(\mathbf{r}) = \frac{4\pi e}{\Delta} \sum_{\mathbf{g} \neq 0} \frac{1}{g^2} \sum_{l=1}^N Z_l S(Z_l, \mathbf{g}) [1 - F(Z_l, \mathbf{g})] e^{-i\mathbf{g}\cdot\mathbf{r}}, \quad (11)$$

where $S(l, \mathbf{g}) = \sum_{j=1}^{N_l} e^{i\mathbf{g}\cdot\mathbf{r}_{j,l}}$, Z_l , $F(Z_l, \mathbf{g})$ are the corresponding structure factors, atomic numbers and atomic form factors; $\mathbf{r}_{j,l}$ and N_l are the corresponding coordinates and number of atoms of the l th species.

Starting from Eq. (11), with the help of basic electrostatic equations, one can obtain physical quantities for an ideal periodic structure, such as the components of the electric field, the electron and atomic densities, i.e., the number of atomic centers per unit of volume.

C. Case of an ideal structure averaged over thermal vibration

Thermal vibrations influence the electric characteristics because of the change in the location of the atoms in the structure [3,21]. As a consequence, we have to approximate the potential by averaging over time and spatial fluctuations: as suggested in the literature [21], we describe the space distribution of atom centers in the primitive cell using normalized probability density functions. In principle, the method allows one to calculate averaged potential for any arbitrary real complex atomic structures. However, in this paper we will work out only the case of isotropic independent thermal oscillations under the assumption that the amplitudes are the same for each atom of a given species. Under this assumption we obtain the three-dimensional potential averaged over thermal fluctuations

$$\varphi(\mathbf{r}) = \frac{4\pi e}{\Delta} \sum_{\mathbf{g} \neq 0} \frac{\langle Y(\mathbf{g}) \rangle}{g^2} e^{-i\mathbf{g}\cdot\mathbf{r}}, \quad (12)$$

where

$$\langle Y(\mathbf{g}) \rangle = \sum_{l=1}^N Z_l S(Z_l, \mathbf{g}) [1 - F(Z_l, \mathbf{g})] e^{-A_l g^2/2}, \quad (13)$$

where A_l is the mean square amplitude of the thermal vibration of the l th species. By the same method we derive the components of the electric field and of the electron and atomic densities averaged out over thermal fluctuations,

$$\mathbf{E}(\mathbf{r}) = \frac{4\pi e i}{\Delta} \sum_{\mathbf{g} \neq 0} \frac{\mathbf{g}}{g^2} \langle Y(\mathbf{g}) \rangle e^{-i\mathbf{g}\cdot\mathbf{r}}, \quad (14)$$

$$\rho_e(\mathbf{r}) = \frac{1}{\Delta} \sum_{l=1}^N Z_l N_l + \frac{1}{\Delta} \sum_{\mathbf{g}} \sum_{l=1}^N Z_l S(l, \mathbf{g}) F(Z_l, \mathbf{g}) e^{-A_l g^2/2} e^{-i\mathbf{g}\cdot\mathbf{r}}, \quad (15)$$

$$\rho_a(\mathbf{r}) = \frac{1}{\Delta} \sum_{l=1}^N N_l + \frac{1}{\Delta} \sum_{\mathbf{g}} \sum_{l=1}^N S(l, \mathbf{g}) e^{-A_l g^2/2} e^{-i\mathbf{g} \cdot \mathbf{r}}. \quad (16)$$

The left side of the equations are real numbers, meaning that the imaginary parts of the complex numbers on the right side are equal to zero.

III. ONE- AND TWO-DIMENSIONAL AVERAGED POTENTIALS

A. Generalities

For interaction of particles with a single crystal, the one- and two-dimensional potentials and their related quantities are widely used [3]. As an example, such approximation can be employed for the study of the cases in which the particles travel between the planes (planar channeling) or parallel to the axes (axial channeling). Thereby, we will average the potential achieved in previous section as a one- and two-dimensional potential. According to the literature [24] we identify planes (hkl) and axes [hkl] through Miller indexes.

B. Orthorhombic and tetragonal lattices

Although previously obtained Eqs. (12)–(16) can be used to describe electrical characteristic of any perfect crystallographic structure, we will focus on the orthorhombic and tetragonal lattice, because the majority of crystals used for channeling have this symmetry or higher. Thus, we choose a Cartesian coordinate system (xyz) with the axes directed along [100], [010], and [001] directions of the crystal. In this coordinate system, we can represent the vector \mathbf{g} in the following form:

$$\mathbf{g} = 2\pi \left(\frac{n_1}{a_1} \mathbf{e}_1 + \frac{n_2}{a_2} \mathbf{e}_2 + \frac{n_3}{a_3} \mathbf{e}_3 \right), \quad (17)$$

where n_1, n_2, n_3 are integer numbers, a_1, a_2, a_3 are the periods of the lattice, $\mathbf{e}_1, \mathbf{e}_2, \mathbf{e}_3$ are the unit vectors along axes of the Cartesian coordinate system.

By using this coordinate system we can define the one- and two-dimensional potentials (also called planar and axial potential, respectively), as follows:

$$\varphi_p(x) = \frac{1}{S_p} \int \int_{S_p} \varphi(x, y, z) dy dz \quad (18)$$

$$\varphi_a(x, y) = \frac{1}{L} \int_0^L \varphi(x, y, z) dz, \quad (19)$$

where S_p is the area of the projection of the primitive cell onto the (100) plane and $L = a_3$ is the period along the z direction. In the same manner, we can obtain $\varphi_p(y), \varphi_p(z)$, for the planar case, and $\varphi_a(x, z), \varphi_a(y, z)$ for the axial case. It is easy to see that averaging out over one or two dimensions brings some simplifications to Eqs. (12)–(16). By taking into account of Eq. (18), the reciprocal vectors sum runs only on n_3 index for the planar case, and runs only on n_2 and n_3 indexes for the axial case. These considerations also affect the scalar product between reciprocal and direct vectors; for

the (100) plane, in planar case, it holds $\mathbf{g} = 2\pi n_1 \mathbf{e}_1/a_1$, $\mathbf{g} \cdot \mathbf{r} = 2\pi n_1 x/a_1$ and for the [100] axis in axial case $\mathbf{g} = 2\pi(n_1 \mathbf{e}_1/a_1 + n_2 \mathbf{e}_2/a_2)$, $\mathbf{g} \cdot \mathbf{r} = 2\pi n_1 x/a_1 + 2\pi n_2 y/a_2$. Channeling in orthorhombic and tetragonal crystals is interesting mostly along major orientations and for that it will not be worked out for the others. The other physical quantities could be either obtained by a similar average or indirectly through the knowledge of the potential.

C. Cubic lattice

In this section we focus on the calculation of the physical quantities of interest for any direction in a cubic lattice because the majority of the crystals used in the experiments have this lattice. We introduce an orthogonal system, with axes defined by $[k_1 k_2 k_3]$, $[l_1 l_2 l_3]$ and $[m_1 m_2 m_3]$ Miller indexes and rewrite Eq. (12) in this coordinate system,

$$\varphi(\mathbf{r}') = \frac{4\pi e}{\Delta} \sum_{\mathbf{g} \neq 0} \frac{\langle Y(\mathbf{g}) \rangle}{g^2} e^{-iG\xi(x', y', z')}, \quad (20)$$

where $G = 2\pi/a$, $\mathbf{g} = G(n_1 \mathbf{e}_1 + n_2 \mathbf{e}_2 + n_3 \mathbf{e}_3)$, a is the side of the cube and with:

$$\xi(x', y', z') = \sum_{i=1}^3 (n_i k_i x' / k_s + n_i l_i y' / l_s + n_i m_i z' / m_s), \quad (21)$$

where $k_s = \sqrt{k_1^2 + k_2^2 + k_3^2}$, $l_s = \sqrt{l_1^2 + l_2^2 + l_3^2}$, $m_s = \sqrt{m_1^2 + m_2^2 + m_3^2}$, and n_i runs from $-\infty$ to $+\infty$.

We also introduce other integer numbers N_1, N_2, N_3 , connected with previous numbers n_1, n_2, n_3 by the relations,

$$n_1 k_1 + n_2 k_2 + n_3 k_3 = N_1, \quad (22)$$

$$n_1 l_1 + n_2 l_2 + n_3 l_3 = N_2, \quad (23)$$

$$n_1 m_1 + n_2 m_2 + n_3 m_3 = N_3. \quad (24)$$

The potential holds

$$\varphi(\mathbf{r}') = \frac{4\pi e}{\Delta} \sum_{\mathbf{g} \neq 0} \frac{\langle Y(\mathbf{g}) \rangle}{g^2} e^{-iG(N_1 x' / k_s + N_2 y' / l_s + N_3 z' / m_s)}. \quad (25)$$

For every fixed number N_1, N_2, N_3 , each individual plane in the crystal lattice is defined by Eqs. (22)–(24) via coefficients $[k_1 k_2 k_3], [l_1 l_2 l_3], [m_1 m_2 m_3]$ [24]. For each selection of the above coefficients, by varying the index N_i all over the set of integer numbers, the whole lying of parallel planes is achieved.

The case when the integer numbers n_1, n_2, n_3 (at fixed N_1, N_2) simultaneously satisfy Eqs. (22) and (23) corresponds to axis along the $[m_1 m_2 m_3]$ direction, thought the inverse proposition does not take place.

The averaged potential along the $[m_1 m_2 m_3]$ axis holds

$$\varphi_a(x', y') = \frac{1}{L} \int_0^L \varphi(x', y', z') dz', \quad (26)$$

where L is the period of potential variation along this axis. It is clear that the average is equivalent to selecting the terms

with $N_3=0$ in the Fourier series. It means that

$$n_1 m_1 + n_2 m_2 + n_3 m_3 = 0. \quad (27)$$

By integrating Eq. (25) we obtain the axial potential along $[m_1, m_2, m_3]$ axis.

$$\varphi_a(x', y') = \frac{4\pi e}{\Delta} \sum_{n_1, n_2 = -\infty}^{+\infty} \frac{\langle Y(n_1, n_2, n_3) \rangle}{g^2} e^{-iG(N_1 x' / k_s + N_2 y' / l_s)}, \quad (28)$$

where n_1, n_2, n_3 numbers are the integer solutions of Eq. (27) and N_1, N_2 are defined by Eqs. (22) and (23).

In a similar manner, one can determine the planar potential for an arbitrary plane of the cubic lattice,

$$\varphi_p(x') = \frac{4\pi e}{\Delta} \sum_{N=-\infty}^{+\infty} \frac{\langle Y(n_1, n_2, n_3) \rangle}{g^2} e^{-iGNk_s x'}, \quad (29)$$

where $n_i = Nk_i$.

IV. PROGRAM FOR CALCULATION OF THE POTENTIAL

Aside from theoretical study in previous section and before we provide examples of calculation of the potential, we describe a program we developed, called ECHARM (Electrical CHARACTERistics of Monocrystals) to enable a nonexpert user for the calculation of the averaged potential of complex atomic structures. The program is free and available at this website [25].

A. Generalities

The ECHARM program is capable of calculating one- and two-dimensional physical quantities of interest averaged out over atomic thermal vibrations. The calculation is limited to the main planes and axes of the orthorhombic and tetragonal cells and to any axes and planes of the cubic cell. The program is written in visual style to aid its usage. Useful section and detailed information are contained in the program helper.

B. Atomic form factors

As in Sec. II B, we will use the single-atomic potential approximation to calculate the potential: as a direct consequence, the correctness of the approximation strongly depends on the atomic form factor chosen, which describes the distribution of the electrons “dressing” the nuclei. In the program three types of approximations are available for atomic form factors, i.e., simple form factor, Molière form factor and experimentally determined form factor.

In the simple form factor approximation, the electrons are distributed in the neighborhood of the nuclei according, in reciprocal space, to the equation

$$F(g) = \frac{1}{1 + g^2 R^2}, \quad (30)$$

where $R = CZ^{1/3} \lambda_c$ (λ_c is Compton length of electron). The constant C is assumed to be 111 in default by the program, though it is possible to modify it.

The Molière approximation is widely adopted in the literature to study channeling because it furnishes a result with comparable accuracy as for analytic calculations [19,20]: the electron density is described, in reciprocal space, by the equation,

$$F(g) = 1 - g^2 \sum_{j=1}^3 \frac{a_j}{b_j^2 + g^2}, \quad (31)$$

where $a_1=0.1, a_2=0.55, a_3=0.35, b_j=Z^{1/3} c_j / (121 \lambda_c), c_1=6, c_2=12, c_3=0.3$.

The experimental form factor represents a precise approximation, which takes into account available data from x-ray measurements, from which one can fit the μ_j, β_j coefficients in the equation,

$$F(g) = \mu_0 + \sum_{j=1}^4 \mu_j e^{-\beta_j g^2}. \quad (32)$$

Lastly, the ECHARM program is equipped with a facility to import x-ray measured electron density.

C. Amplitude of thermal vibrations

The amplitude of thermal vibrations is important at each temperature, therefore the ECHARM program gives the flexibility to set its value manually, allowing the user to introduce x-ray measurement of the root mean square of thermal vibration amplitude, or it allows to calculate it from Debye temperature.

We expect that the energy of thermal vibrations remains the same for any atomic species [24], meaning that the root mean square of the amplitude is inversely proportional to the atomic mass.

V. EXAMPLES OF CALCULATIONS

A. Simple structures

Nowadays, the crystals that have best performed in channeling experiments were made of silicon. The calculation of the potential in these crystals was achieved by several analytical methods, and, in particular, with the Molière model for the atomic form factor, as estimated in Ref. [6].

As a first test bench for the ECHARM program, we will calculate the potential in silicon through Molière approximation and compare the results with those in the literature. Second, the refinement given by including the electron density as measured by x-ray experiments will be shown.

We determined the planar potential in the case of silicon for the strongest orientations, i.e., (111) and (110), as depicted in Fig. 1. One observes the typical two-well shape for (111) orientation with a large (l) and a small (s) wells, whose maximum depth is $U_0=25.68$ eV (l), and a single well for (110) orientation ($U_0=23.39$ eV). The same quantities were calculated for germanium, $U_0=41.82$ eV and $U_0=40.67$ eV for (111) and (110) orientations, respectively.

By replacing the Molière approximation with the experimentally achieved form factor by x-ray diffraction [26,27], we obtained a decrease in the potential barrier height by less

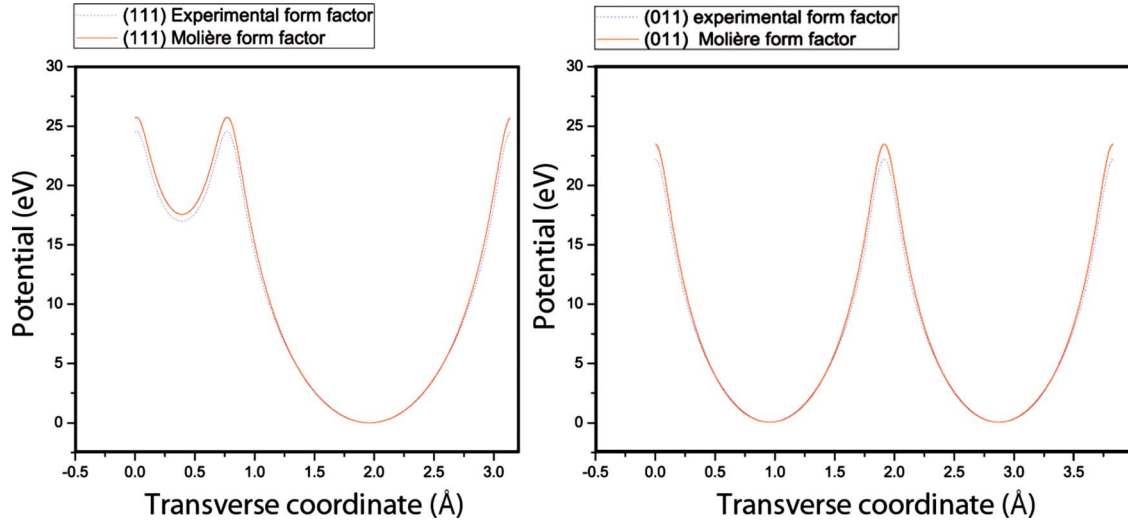


FIG. 1. (Color online) Calculation of potential between (111) planes and (110) planes in Si with Moliere atomic form factor and the form factor achieved by x-ray experiments. The potential calculated with the latter method is lower than for the former method, especially in proximity of the atomic planes.

than 10%, though the same shape of the potential held (Fig. 1). For comparison, it turned out $U_0=22.55$ eV and $U_0=21.38$ eV for (111)(l) and (110) orientations, respectively. A recent experiment [28] showed a better agreement of the experimental results with such calculation of U_0 instead of the determinations based on Molière approximation.

We also determine the axial potential depths for [111] ($U_0=117$ eV) and [011] ($U_0=152$ eV) directions in a silicon crystal, which are in good agreement with the estimates in Ref. [3] ($U_0=106$ eV and $U_0=140$ eV, respectively) and in fair agreement with Ref. [6] ($U_0=105$ eV and $U_0=114$ eV, respectively). This discrepancy owes to the contribution of all axes to the potential as is in our case while other methods accounts for only neighboring axes.

Lastly, we carried out the detailed comparison of our method with the method based on the analytical expression of the Moliere potential (see [6,16,19,20]). Usually, in this method the potential is calculated in approximation of the two neighboring crystallographic planes. We denote this approximation as $\varphi_{2p}(x)$. For our aims we calculate with the help of this method potential of the (110) silicon plane taking into account the contribution from four and six neighboring planes ($\varphi_{4p}(x)$, $\varphi_{6p}(x)$ approximations, correspondingly).

The results of this comparison are presented in the Table I. Note, the calculations were done with usage of the two methods at the same conditions, in particular at the same rms

amplitude of thermal vibration and screening radius. The calculations corresponds to temperature of single crystal equal to 300 K. For comparison we present in the table results of calculation for potential $\varphi_X(x)$, which was obtained in x-ray measurements. We also present the calculation of the Molière potential for the case when amplitude of the thermal vibration is equal to zero (so called static potential). We denote this potentials as $\varphi_{2pS}(x)$ and $\varphi_{MS}(x)$ and they were obtained similar as $\varphi_{2p}(x)$ and $\varphi_M(x)$ potentials.

We see that the potential $\varphi_{6p}(x)$ is very close to potential $\varphi_M(x)$ which was calculated with the help of Eq. (11). We can conclude that the both methods give the same result, as expected.

Besides, we see that $\varphi_{2p}(x) < \varphi_{6p}(x) \approx \varphi_M(x)$ at $|x| > 0$. The largest difference between potentials takes place at $x = 1$ and equal to ≈ 0.9 eV or 4% of the absolute value of the potential $\varphi_{6p}(x)$.

B. Complex structures: Zeolites

Zeolites are largely studied materials because of their widespread applications, spanning from heterogeneous catalysis to gas purification [29]. A natural zeolite is an alumino-silicate framework, whose structure contains cavities filled with water and exchangeable cations. The primary buildings units of the structures of silicates are the TO4 tet-

TABLE I. Different calculations of potential of the (110) silicon plane as a function of relative coordinate $\nu=2x/d$, where d is the interplanar distance. The point $x=0$ corresponds to a minimum of the potential.

$\nu=2x/d$	$\varphi_{2p}(\nu)$	$\varphi_{4p}(\nu)$	$\varphi_{6p}(\nu)$	$\varphi_M(\nu)$	$\varphi_X(\nu)$	$\varphi_{2pS}(\nu)$	$\varphi_{MS}(\nu)$
0.2	0.605	0.633	0.635	0.635	0.623	0.598	0.628
0.4	2.545	2.662	2.668	2.669	2.550	2.513	2.635
0.6	6.329	6.601	6.615	6.617	6.043	6.224	6.510
0.8	13.421	13.930	13.956	13.959	12.469	13.104	13.639
1.0	22.465	23.313	23.356	23.360	21.383	27.577	28.466

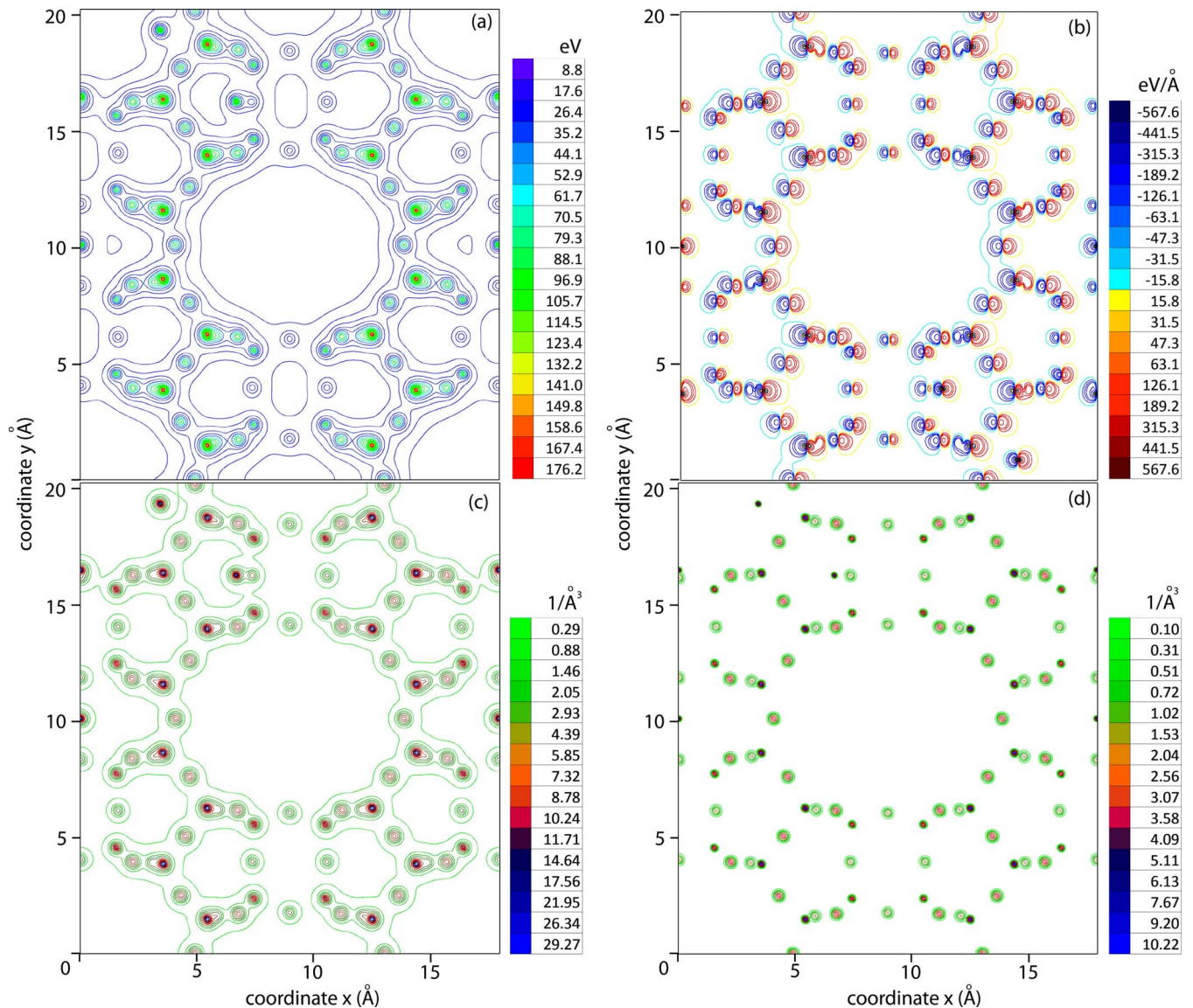


FIG. 2. (Color online) Contour plot of physical quantities of interest along the [001] axis of Mordenite at $T=300$ K, as a function of coordinate x and y . (a) Potential: a wide channel with uniform potential is visible on the center of the figure. The ion breaking the symmetry of the potential are Ca^{++} cations bound to the well of the channel. (b) Electric field (x component). (c) Electron density. (d) Atomic density: this figure gives a picture of the extent of the atomic oscillations in the crystal.

rahedra, where T is mainly Si. The extraframework cations in the structure (usually K, Na, Ca, less frequently Li, Mg, Sr, Ba) often result in significant change of both physical and chemical properties. Under some circumstances, neighboring cavities merge to form long channels, which are periodically repeated over the whole structure and may form a bundle of parallel nanotubes. These crystals are ideal cases for particle capture via axial channeling. Moreover, the knowledge of precise data about the potential in zeolites allows to design experiments about Coulomb explosions of charged molecules in crystals. Pioneering experiment in this sense has been carried out in silicon crystal [30], though the wide channels offered by a zeolite should increase the efficiency of the method. Among the immensely wide variety of zeolites, we selected the species that possess broad channels, good thermal stability and, ultimately, that exist as relatively large crystals to be used for experiments.

The first sample we simulated is mordenite [29,31,32], whose potential, electric field, atomic density and density of electrons along the [001] axis are illustrated in Fig. 2. The crystal lattice is orthorhombic ($a_1=18.007$ Å, $a_2=20.269$ Å, $a_3=7.465$ Å) and Si, Al and O atoms form its base. In order to simulate the structure of mordenite closer to the existing crystals of this kind, we added Ca cations to the framework in the locations at which such ions are bound to the framework. The profile of the potential very much resembles the structure of the zeolite and exhibits nearly a field-free 14 eV deep channel, extending roughly 9 Å in diameter. The depth of the potential well is comparable to that of silicon.

The second sample we simulated is boggsite [33], whose potential, electric field, atomic density and density of electrons along the [100] axis are illustrated in Fig. 3: the crystal lattice is orthorhombic ($a_1=20.041$ Å, $a_2=23.814$ Å, a_3

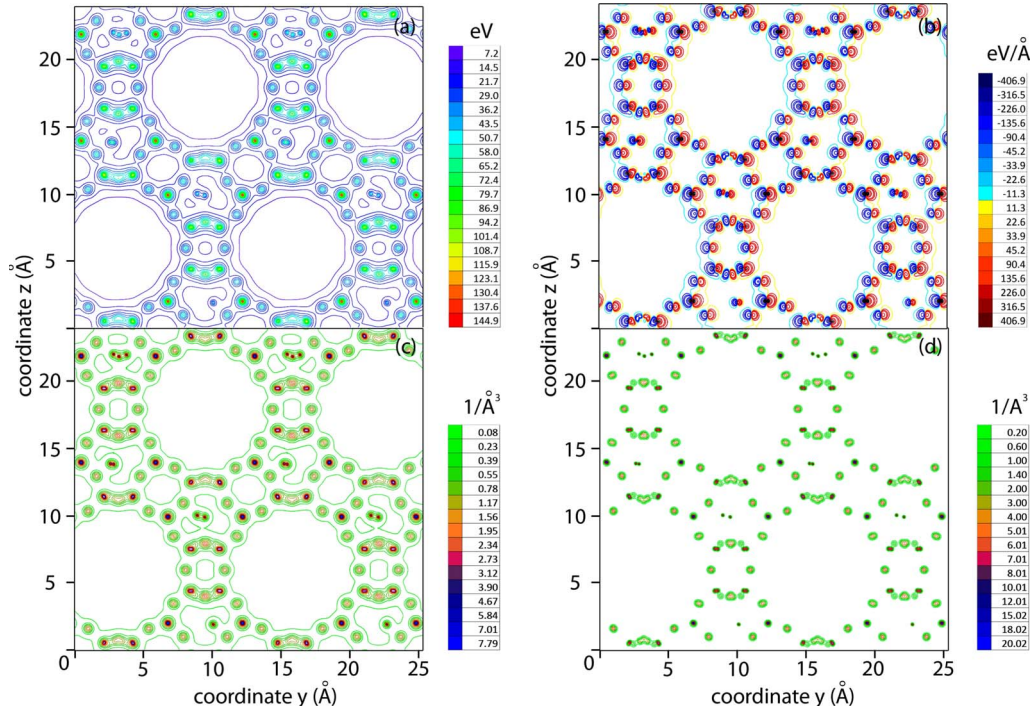


FIG. 3. (Color online) Contour plot of physical quantities of interest along the [100] axis of Boggsite at $T=300$ K, as a function of coordinate y and z . (a) Potential. (b) Electric field (x component). (c) Electron density. (d) Atomic density.

$=12.869$ Å) and the base is composed by Si, Al, Ca, and O atoms. Boggsite shows impressive thermal stability [34], which gives the possibility to heat the sample and remove the water molecules absorbed in its channels without significant structure deformation. Boggsite exhibits two interesting large channels for axial channeling, a channel with a 12-atom perimeter along [100] direction, a channel with a 10-atom perimeter along [010] direction. Each direction highlights a deep well (14 eV for [010] and 14.5 eV for [100]), i.e., two interesting situations for axial channeling of positively charged particles.

Another important feature of zeolites crystals is the negligible density of electrons inside the channels, as shown in Fig. 3 for the particular case of boggsite. Indeed, scattering processes between channeled particles and atomic electrons lead to dechanneling, which is thereby considerably weakened for a zeolite.

C. Cubic structure: silicon and silicon carbide

The interplanar potentials of silicon (001), (011), and (111) planes were calculated and studied to explain the behavior of channeled particles in oriented crystals [3,6,20] and to furnish important information about the depth of the po-

tential well and, in turn, the critical angle for channeling and the other fundamental physical quantities.

Apart from such major planes in silicon, rather modest information is available for channeling in minor orientations. Indeed, a recent experiment [7] showed the transition from the stable confinement of axially channeled particles toward planar channeling of minor orientations, this effect being the limiting factor for particle steering via axial channeling. Thus, the knowledge of the potential of such minor orientations for planar channeling is demanded.

Another effect involving minor orientations is for the case of multivolume reflection in a single crystal [35], i.e., an effect in which the contributions of all the orientations sharing a common axis add up to deflect the particles.

As an example, we show several planes with high-order indexes in a silicon crystal (see Table II) and calculate their potential energy.

A crystalline material with cubic symmetry that deserves special attention is SiC. Its elevated melting point together with the high perfection of available crystals of this kind suggests the application under high particle fluxes. To prove the versatility of the algorithm of calculation we determined the potential and electric field in axial mode along the [112] axis, as illustrated in Fig. 4 respectively.

TABLE II. Potential well depth (U_0) and interplanar distance (D) for several high-order planes in silicon crystal: all the values are evaluated using the experimentally achieved form factor.

Plane	(201)	(211)	(221)	(301)	(311)(l)	(321)	(331)(l)	(332)
D (Å)	0.61	1.11	0.45	0.85	1.23	0.73	1.00	0.58
U_0 (eV)	2.89	8.64	1.48	5.54	9.35	4.09	6.02	2.62

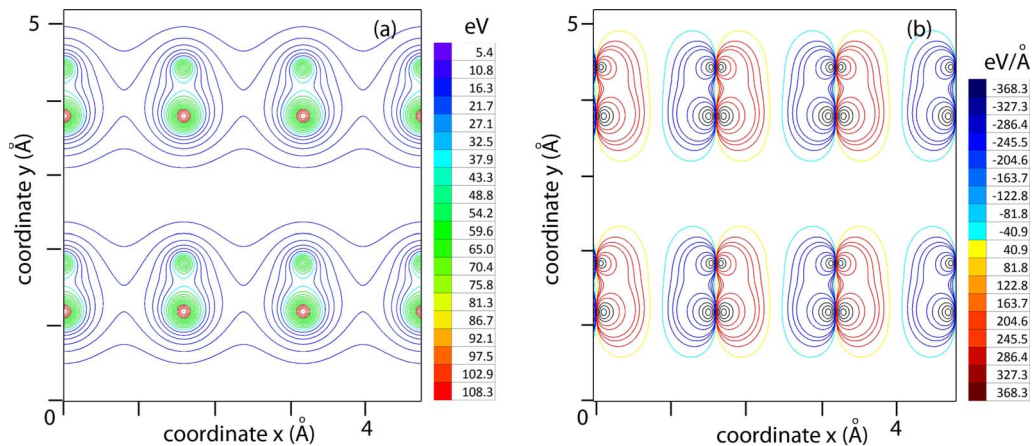


FIG. 4. (Color online) Potential (a) and electric field (b) in the axial case along the $[112]$ axis for a SiC at $T=297$ K.

VI. DISCUSSION AND CONCLUSIONS

We have developed a method for calculation of the potential and related physical quantities for investigation of interaction of particles with oriented crystals. The method relies on a Fourier expansion of the potential in a periodic structure. The advantages of such an approach are that the calculation is made over the whole crystal atoms and x-ray data measurements can be imported to calculate atomic form factor. The algorithm exhibits maximal flexibility for the cubic symmetry and allows to calculate the physical quantities of interest for complex structure. In the calculation, perturbing effects of external electromagnetic fields are not considered as well as the delocalization of electrons is neglected.

The algorithm has been developed specifically for the most interesting cases for planar and axial channeling, i.e., orthorhombic and tetragonal crystals along major directions, and any direction for the cubic lattice. We provided examples of calculation in complex structures, such as zeolites, and show the corrections due to the usage of atomic form factors achieved by measurements with x-ray experiments and compare to previously existing models.

We finally wrote the ECHARM program, i.e., a free software for calculation of the physical quantities described in

this paper. Calculation time strictly depends on the structure, as an example the determination of the potential of Boggsite (Fig. 3) took approximately 2 h with a standard personal computer. For this reason we limited the number of atomic species to 50 with 1000 atoms per species.

The ECHARM program is intended to aid the design of new crystals for experiments. As an example, the characteristics of new materials for channeling experiments can be simulated before the experiments even in the case of complex structure such as zeolite. At low energy, the ECHARM program could be implemented as a routine in the software for analysis of Rutherford backscattering spectroscopy, especially for operation in channeling mode, for better description of experimental energy spectra of backscattered particles.

We believe that the program can be of widespread application in several areas.

ACKNOWLEDGMENTS

We would like to thank A. Alberti for useful information about zeolites. We acknowledge financial support by INFN-COHERENT project and by MIUR Project No. 2008TMS4ZB. This work was partially supported by RFBR Grant No. 08-02-01453-a.

-
- [1] M. Sugawara, *Plasma Etching: Fundamentals and Applications* (Oxford University Press Inc., New York, 1998).
- [2] Y. E. Shalom Eliezer, *Plasma Physics and Fusion Energy* (Cambridge University Press, Cambridge, England, 2008).
- [3] V. Baier, V. Katkov, and V. Strakhovenko, *Electromagnetic Processes at High Energies in Oriented Single Crystals* (World Scientific Publishing, Singapore, 1998).
- [4] V. I. Vysotskii and R. N. Kuz'min, *Sov. Phys. Usp.* **35**, 725 (1992).
- [5] U. I. Uggerhøj, *Rev. Mod. Phys.* **77**, 1131 (2005).
- [6] V. Biryukov, Y. Chesnekov, and V. Kotov, *Crystal Channeling and Its Applications at High-Energy Accelerators* (Springer, New York, 1996).
- [7] W. Scandale, A. Vomiero, S. Baricordi, P. Dalpiaz, M. Fiorini, V. Guidi, A. Mazzolari, G. D. Mea, R. Milan, G. Ambrosi *et al.*, *Phys. Rev. Lett.* **101**, 164801 (2008).
- [8] W. Scandale, D. A. Still, A. Carnera, G. D. Mea, D. D. Salvador, R. Milan, A. Vomiero, S. Baricordi, P. Dalpiaz, M. Fiorini *et al.*, *Phys. Rev. Lett.* **98**, 154801 (2007).
- [9] Y. Okazaki, M. Andreyashkin, K. Chouffani, I. Endo, R. Hamatsu, M. Iinuma, H. Kojima, Y. P. Kunashenko, M. Masuyama, T. Ohnishi *et al.*, *Phys. Lett. A* **271**, 110 (2000).
- [10] V. A. Maisheev, e-print arXiv:hep-ex/9904029.
- [11] V. Biryukov and S. Bellucci, *Nucl. Instrum. Methods Phys. Res. B* **234**, 99 (2005), relativistic channeling and related coherent phenomena in strong fields.

- [12] C. Biino, M. Clement, N. Doble, K. Elsener, A. Freund, L. Gatignon, P. Grafström, K. Kirsebom, U. Mikkelsen, S. P. Møller *et al.*, Phys. Lett. B **403**, 163 (1997).
- [13] T. Suwada, M. Satoh, K. Furukawa, T. Kamitani, T. Sugimura, K. Umemori, H. Okuno, Y. Endou, T. Haruna, R. Hamatsu *et al.*, Phys. Rev. ST Accel. Beams **10**, 073501 (2007).
- [14] X. Artru, S. Fomin, N. Shul'ga, K. Ispirian, and N. Zhevago, Phys. Rep. **412**, 89 (2005).
- [15] S. Bellucci and V. Maisheev, Nucl. Instrum. Methods Phys. Res. B **234**, 87 (2005).
- [16] W. K. Chu, W. R. Allen, S. T. Picraux, and J. A. Ellison, Phys. Rev. B **42**, 5923 (1990).
- [17] J. Lindhard, K. Dan. Vidensk. Selsk. Mat. Fys. Medd. **34**, 14 (1965).
- [18] C. Erginsoy, Phys. Rev. Lett. **15**, 360 (1965).
- [19] B. R. Appleton, C. Erginsoy, and W. M. Gibson, Phys. Rev. **161**, 330 (1967).
- [20] D. S. Gemmell, Rev. Mod. Phys. **46**, 129 (1974).
- [21] S. Bellucci and V. A. Maisheev, Phys. Rev. B **71**, 174105 (2005).
- [22] V. Maisheev, V. Mikhalev, and A. Frolov, Sov. Phys. JETP **74**, 740 (1992).
- [23] V. Maisheev, Nucl. Instrum. Methods Phys. Res. B **119**, 42 (1996).
- [24] C. Kittel, *Introduction to Solid State Physics*, 8th ed. (Wiley, New York, 2005).
- [25] E. Bagli, V. Guidi, and V. Maisheev, www.fe.infn.it/echarm
- [26] D. Cromer and J. Waber, Acta Crystallogr. **18**, 104 (1965).
- [27] D. Cromer and J. Waber, Acta Crystallogr. **19**, 224 (1965).
- [28] W. Scandale, A. Vomiero, S. Baricordi, P. Dalpiaz, M. Fiorini, V. Guidi, A. Mazzolari, R. Milan, G. D. Mea, G. Ambrosi *et al.*, Phys. Rev. Lett. **101**, 234801 (2008).
- [29] G. Gottardi, *Natural Zeolites* (Springer-Verlag, Berlin, 1985).
- [30] R. González-Arrabal, V. Khodyrev, N. Gordillo, G. García, and D. Boerma, Nucl. Instrum. Methods Phys. Res. B **249**, 65 (2006).
- [31] W. M. Meier, Z. Kristallogr. **115**, 439 (1961).
- [32] A. Alberti, Am. Mineral. **64**, 1188 (1979).
- [33] S. J. V. Pluth Joseph, Am. Mineral. **75**, 501 (1990).
- [34] A. A. Stefano Zanardi, Giuseppe Cruciani, and E. Galli, Am. Mineral. **89**, 1033 (2004).
- [35] V. Tikhomirov, Phys. Lett. B **655**, 217 (2007).